# Soluble Melanoma Cell Adhesion Molecule (sMCAM/sCD146) Promotes Angiogenic Effects on Endothelial Progenitor Cells through Angiomotin*

Jimmy Stalin[‡1], Karim Harhouri[‡1], Lucas Hubert[‡], Caroline Subrini[‡], Daniel Lafitte[§], Jean-Claude Lissitzky[¶], Nadia Elganfoud[‡], Stéphane Robert[‡], Alexandrine Foucault-Bertaud[‡], Elise Kaspi[‡], Florence Sabatier[‡], Michel Aurrand-Lions[¶], Nathalie Bardin[‡], Lars Holmgren[‖], Françoise Dignat-George[‡], and Marcel Blot-Chabaud[‡2]

From [‡]Inserm UMR-S 1076, Physiopathology of Endothelium, Aix-Marseille University, Formation and Research Unit of Pharmacy, 13005 Marseille, France, [§]Inserm UMR 911, Research Center in Biological Oncology and Oncopharmacology, Proteomic Platform, Aix-Marseille University, 13005 Marseille, France, [¶]Inserm U1068, Research Center in Cancerology of Marseille, Aix-Marseille University, 13009 Marseille, France, and the [‖]Department of Oncology and Pathology, Cancer Centrum Karolinska, Karolinska Institut, SE17176 Stockholm, Sweden

**Background:** Soluble melanoma cell adhesion molecule (sMCAM/sCD146) promotes angiogenic effects on endothelial progenitor cells (EPC).
**Results:** sCD146 binds angiomotin in EPC and triggers the activation of different signaling pathways. Silencing angiomotin prevents this activation and angiogenic effects.
**Conclusion:** Angiomotin is identified as a novel binding partner of sCD146.
**Significance:** Angiomotin mediates the angiogenic effects of sCD146.

The melanoma cell adhesion molecule (CD146) contains a circulating proteolytic variant (sCD146), which is involved in inflammation and angiogenesis. Its circulating level is modulated in different pathologies, but its intracellular transduction pathways are still largely unknown. Using peptide pulldown and mass spectrometry, we identified angiomotin as a sCD146-associated protein in endothelial progenitor cells (EPC). Interaction between angiomotin and sCD146 was confirmed by enzyme-linked immunosorbent assay (ELISA), homogeneous time-resolved fluorescence, and binding of sCD146 on both immobilized recombinant angiomotin and angiomotin-transfected cells. Silencing angiomotin in EPC inhibited sCD146 angiogenic effects, *i.e.* EPC migration, proliferation, and capacity to form capillary-like structures in Matrigel. In addition, sCD146 effects were inhibited by the angiomotin inhibitor angiostatin and competition with recombinant angiomotin. Finally, binding of sCD146 on angiomotin triggered the activation of several transduction pathways that were identified by antibody array. These results delineate a novel signaling pathway where sCD146 binds to angiomotin to stimulate a proangiogenic response. This result is important to find novel target cells of sCD146 and for the development of therapeutic strategies based on EPC in the treatment of ischemic diseases.

CD146 is a junctional adhesion molecule belonging to the immunoglobulin superfamily, which contains a proteolytic variant detectable in the human serum (sCD146).[3] The level of this soluble form has been shown to be modulated in different pathologies, such as inflammatory bowel diseases (1), pathological pregnancies (2), or chronic renal failure (3). However, until recently, its physiological role was unknown. In a previous report, we have shown that sCD146 is involved in inflammation by specifically binding to monocytes and thereby stimulating transendothelial migration (4). We have further shown that sCD146 is also involved in angiogenesis (5). Thus, sCD146 exhibited chemotactic activity on different cell types involved in vessel formation, as smooth muscle cells and endothelial cells, including progenitor endothelial cells (EPC). In addition, treatment of EPC with sCD146 led to an increased migration, proliferation, and capacity to form capillary-like structures in Matrigel (5), suggesting the presence of a membrane-associated binding partner of sCD146 on endothelial cells. Finally, using an animal model of hind limb ischemia, we showed that local treatment with sCD146 led to the recruitment of EPC and to an increase in blood flow and neovessel formation (5).

Although sCD146 was described a few decades ago, its endothelial binding partner and its intracellular signaling pathways are still unknown. It has been reported that CD146 functioned as a homophilic adhesion molecule, suggesting a possible interaction between sCD146 and membrane CD146. However, to the best of our knowledge, biochemical evidence for homophilic interaction is lacking. Using different approaches, including surface plasmon resonance (4), we were unable to demonstrate an interaction between soluble and membrane CD146.

[3] The abbreviations used are: sCD146, soluble CD146; EPC, endothelial progenitor cell(s); Amot, angiomotin; HTRF, homogeneous time-resolved fluorescence; rsCD146, recombinant soluble CD146; HUVEC, human umbilical vein endothelial cell(s); EBM-2, endothelial basal medium 2; Fak, focal adhesion kinase; Icos, inducible co-stimulatory; eNOS, endothelial nitric oxide synthase.

These results led us to hypothesize that sCD146 does not interact with membrane CD146 but with an unidentified membrane-associated protein. This hypothesis was also supported by the fact that sCD146 binds monocytes (4), which do not express CD146. In this study, we have used peptide pulldown of sCD146 in EPC lysates to identify potential target proteins. We present evidence that the proangiogenic effects of sCD146 are mediated via its binding to angiomotin.

## EXPERIMENTAL PROCEDURES

*Peptide Pulldown and Mass Spectrometry*—Peptide pulldown experiments were performed using recombinant sCD146 (rsCD146) as a bait in an EPC lysate under non-denaturing conditions. After electrophoresis, proteins were identified by peptide mass fingerprinting and MALDI mass spectrometry as described previously (6).

*ELISA*—To examine interaction between sCD146 and angiomotin, an ELISA was developed. Angiomotin (1 $\mu$g/well) capture was explored using a solid phase absorbed rsCD146 at 1 $\mu$g/well. Icos receptor (1 $\mu$g/well) was used as a control. Anti-angiomotin, anti-CD146, or anti-Icos receptor antibodies coupled to anti-HRP antibody were used to reveal the interaction.

*Homogeneous Time-resolved Fluorescence (HTRF) assay*—The HTRF assay was performed according to a protocol from CisBio Bioassays (Codolet, France). The following reagents were added sequentially into a 96-well half-area plate: 25 $\mu$l of control or serially diluted rsCD146/angiomotin solutions in PBS-BSA 0.2% as indicated, 25 $\mu$l of anti-GST-europium cryptate, and 25 $\mu$l anti-Myc-d2. Reactions in a final volume of 100 $\mu$l were incubated overnight at 4 °C before reading the HTRF signals using a microplate reader (Polarscan; BMG Labtech).

*Cell Culture of HUVEC and EPC*—Human umbilical vein endothelial cells (HUVEC) were prepared from human umbilical cord samples collected in compliance with French legislation as described previously (4). Late EPC were prepared from human umbilical cord blood samples collected from donors, in compliance with French legislation as described previously (5, 7). Briefly, cord blood mononuclear cells were isolated by density gradient centrifugation. They were then preplated in RPMI/10% fetal calf serum for 24 h in plastic flasks before nonadherent cells were isolated and grown in culture. Both EPC and HUVEC were plated onto collagen-coated well plates and maintained in endothelial basal medium 2 (EBM-2) supplemented with EGM-2 SingleQuots (EGM-2 medium (Clonetics, Walkersville, MD). For expansion of EPC and HUVEC, colonies were trypsinized, and cells were replated on plates or Lab-Tek slides depending on the experiment. Cells were maintained under standard conditions (humidified atmosphere, 5% $CO_2$, 37 °C) and used non-confluent (migratory phenotype) in the experiments. In stimulation experiments, cells were starved for 3 h in EBM-2 and then stimulated with either rsCD146 or recombinant human angiostatin as a function of the experiment.

*Endothelial Cell Tube Formation in Matrigel*—The 96-well plates were precoated with 1:1 mixture of cold Matrigel Basement Membrane (10 mg/ml, BD Biosciences): EBM-2 medium. After 45 min of polymerization at 37 °C, EPC were plated at $10^4$ cells/well in EBM-2 supplemented or not with rsCD146. After

6 h, pictures of representative fields were taken for each condition under an inverted microscope at 400× magnification. Capillary tube formation was evaluated by measuring the total number of tubes per field with the Lucia software (Nikon).

*Cell Proliferation Assay*—EPC were seeded on 96-well plates ($5.10^3$/well) and cultured in EGM-2 medium for 3 days. Cells were then preincubated for 2 h in EBM-2 medium. Cell proliferation was assayed by 5-bromo-2′-deoxy-uridine (BrdU) incorporation into cellular DNA using the BrdU labeling and detection kit III (Roche Applied Science). In brief, cells were incubated 12 h with BrdU-labeling solution in EBM-2 medium in the absence or presence of rsCD146 and fixed. Cellular DNA was partially digested by nuclease treatment, and incorporated BrdU was detected with a peroxidase-conjugated anti-BrdU primary antibody. The absorbance was measured at 450 nm using a microplate reader. Results were expressed as arbitrary units. Experiments were performed in triplicates.

*Wound Healing Assay*—A reproducible wound was performed with a pipette tip on a confluent monolayer of EPC cultured on 24-well plates. The surface of the wound was measured at 400× magnification using an Olympus inverted microscope and acquired with the Biocom Visiolab image analysis software (Les Ulis, France). The medium was removed, and EPC were incubated for 6 h with EBM-2 medium containing or not rsCD146. Cell wound repair was calculated by subtracting the wound area measured after 6 h of incubation with rsCD146 from the area of the original wound. Results were expressed as a percentage of the area of the original wound, considered as 100%.

*Immunofluorescence Experiments*—EPC were fixed with 3% formaldehyde in PBS for 30 min at room temperature and permeabilized or not with 0.2% Triton X-100 as a function of the experiments. After washing with PBS and incubation with blocking reagent (5% BSA in PBS) for 15 min, cells were labeled with rsCD146-FITC, angiostatin was coupled to an anti-angiostatin Ab and secondary FITC-labeled Ab and irrelevant IgG1-FITC Ab (20 $\mu$g/ml) without permeabilization, or anti-angiomotin mAb (20 $\mu$g/ml) and secondary FITC-labeled Ab after permeabilization. The samples were mounted in Mowiol and examined with a Leica microscope.

*Flow Cytometry Experiments*—The level of membrane expression of CD146 was determined on HUVEC and EPC as described previously (5). All detached endothelial cells were labeled for 1 h at 4 °C with rsCD146-FITC (1.5 $\mu$M), angiostatin (1.5 $\mu$M) coupled to an anti-angiostatin Ab, and secondary FITC-labeled Ab and/or irrelevant IgG1-FITC Ab (1.5 $\mu$M). In some experiments, HUVEC or EPC were labeled in the presence of 1.5 $\mu$M angiostatin. After washing, samples were analyzed by flow cytometry on a Beckman Coulter apparatus (FC 500). Flow cytometry experiments were also performed on a construct consisting of magnetic beads (Dynabeads; Invitrogen) coupled to an anti-GST antibody (Sigma-Aldrich) and recombinant (rAmot) coupled through its GST tag. The binding of rsCD146-FITC (1.5 $\mu$M) was evaluated as described above.

*Protein Expression Profiling*—Total cell lysates were prepared from cultured late EPC treated or not for 24 h with 50 ng/ml rsCD146. Antibody arrays were performed according to

the manufacturer's instructions (Tebu-Bio; Le Perray en Yvelines; France). Spot signals were quantified using the Tebu-Bio software. Subtraction of background was done for the signal mean intensities in both test and reference spots.

*Quantitative RT-PCR*—Total cellular RNA was isolated from late EPC using the RNeasy kit (Qiagen GmbH, Hilden, Germany) according to the manufacturer's instructions, including the DNase digestion step. 5 $\mu$g of total RNA were reverse-transcribed into cDNA in a 50-$\mu$l reaction containing 40 units of RNaseOUT (Invitrogen), 150 ng of random hexamers (Roche Applied Science), 10 mM dNTPs (Invitrogen), and 200 units of Superscript II (Invitrogen). The resulting cDNA was diluted 1:80 and was subjected to quantitative PCR using primer sets specific for the gene or control gene at an optimized oligonucleotide concentration of 200 nM. Forward and reverse specific primer sequences for eNOS and GAPDH were as follows: forward, 5′-CTCATGGGCACGGTGATG-3′ and reverse, 5′-ACCACGTCATACTCATCCATACAC-3′; forward, 5′-GGTGGTCTCCTCTGACTTCAACA-3′ and reverse, 5′-GTTGCTGTAGCCAAATTCGTTGT-3′, respectively. Reactions were performed in a total volume of 20 $\mu$l using the Full Velocity hot start SYBR Green Quantitative PCR Mastermix according to the manufacturer's instructions (Stratagene). Amplification cycles were as follows: one denaturation cycle of 5 min at 95 °C, followed by 40 amplification cycles of 10 s at 95 °C and 30 s at 60 °C. Amplification, data acquisition, and analysis were performed using the Mx3000P instrument and the Mx300P software (version 2.0; Stratagene). The threshold cycle ($C_t$) for each gene was normalized to that of GAPDH.

*Western Blot Experiments*—Western blot analysis was performed as described previously (4, 5). Briefly, cells were grown on plates treated or not for 24 h with rsCD146 50 ng/ml and then washed in PBS, scraped off of the plates, and extracted with 300 $\mu$l of ice-cold lysis buffer (150 mM NaCl, 50 mM Tris HCl (pH 7.4), 2.4 mM EDTA, 1% Nonidet P40, 0.5 mM phenylmethylsulfonyl fluoride) for 30 min at 4 °C. After centrifugation (12,000 × $g$, 10 min, 4 °C) to eliminate cell debris and nuclei, proteins were quantified by protein assay (BCA protein assay kit, Pierce). 50 $\mu$g of protein were mixed with NuPAGE lithium dodecylsulfate sample buffer (Invitrogen) and NuPAGE sample-reducing agent (Invitrogen). Samples were then subjected to NuPAGE using 4–12% Novex Bis-Tris gels (Invitrogen), and separated proteins were transferred onto nitrocellulose membranes (Invitrogen). Membranes were probed with specific primary antibodies (anti-p-Fak, anti-p-Jnk, anti-p-Akt, anti-Akt, anti-p-p38, anti-p38 diluted 1/1000 or anti-actin diluted 1/5000) followed by secondary antibodies coupled to peroxidase. Blots were revealed with the ECL substrate (Pierce). Membranes probed with various antibodies were stripped between antibodies.

In a particular experiment, plasma membranes were isolated from EPC or HUVEC using the Mem-Per eukaryotic membrane protein extraction kit (Perbio; Brebières, France). Western blot experiments were then performed as described above with anti-angiomotin (1/500), anti-pecam-1 (1/1000), anti-lamin A/C (1/1000), and anti-grasp55 (1/500) antibodies.

*siRNA and Transfection Experiments*—Specific small interfering RNA (siRNA) experiments were performed as described previously (8) to suppress expression of angiomotin. The Amaxa nucleofection kit (HUVEC old nucleofactor kit; Lonza; Cologne, Germany) was used as described by the manufacturer. Approximately 85–90% of the EPC were transfected as attested by control experiments with a plasmid encoding GFP (data not shown). EPC were plated in Petri dishes after transfection, and adherent living cells were used 48 h after transfection for *in vitro* experiments. Efficiency of siRNA transfection was tested by Western blot (see "Results").

A plasmid encoding the angiogenic isoform of angiomotin (p80) in a pcDNA3 expression vector was also transfected into HeLa cells, which do not express the protein, using the Amaxa nucleofection kit. Transfected cells were used 48 h after transfection for *in vitro* studies. Efficiency of CD146 overexpression was verified by Western blot (see "Results").

*Peptides, Antibodies, Inhibitors, and siRNA*—Recombinant human forms of soluble CD146 (Myc-tagged), recombinant angiomotin (p80 isoform; GST-tagged), angiostatin, and Icos receptor were obtained from Biocytex, Abnova, and Cell Sciences, respectively. Anti-angiomotin (Abnova), anti-angiostatin (Sigma Aldrich), anti-pecam 1 (Santa Cruz Biotechnology), anti-lamin A/C (Santa Cruz Biotechnology), and anti-grasp55 (Abnova) antibodies were used. Anti-p-Fak, anti-p-Jnk, anti-p-Akt, anti-Akt, anti-p-p38, and anti-p38 antibodies were from Cell Signaling. siRNA specific for angiomotin were used (Invitrogen) (GAGAACACCCGUGAGAGAGACUUG/UCAAGUCUCUCUCACGGGUGUUCUC). Fak inhibitor 14 and Akt inhibitor (GSK690693) were from Santa Cruz Biotechnology.

*Statistical Analysis*—Data were expressed as mean ± S.E. Statistical analysis and curve fits and analysis were performed with Prism software (GraphPad Software, Inc., San Diego, CA).

## RESULTS

*Interacting Partners of Soluble CD146*—Proteins obtained by peptide pulldown using rsCD146 as a bait in a non-denaturating lysate of EPC were analyzed by mass spectrometry. Five proteins were identified: $\beta$-actin, filamin $\beta$2, HSP70, HSP90, and angiomotin. We focused on angiomotin because of its documented role in angiogenesis and because it was the only membrane-associated protein identified.

*Interaction between sCD146 and Angiomotin*—A series of experiments were performed to confirm the interaction between angiomotin and soluble CD146. ELISA revealed that rAmot was effectively able to bind rsCD146, whereas an irrelevant protein (Icos Receptor) was not (Fig. 1*A*).

These results were confirmed by HTRF assay. A dose-dependent binding of rsCD146 was observed on angiomotin (Fig. 1*B*). The estimated dissociation constant obtained from the Scatchard plot (Fig. 1, *inset*) was $1.05 \times 10^{-7}$ M. This binding was specific because it was completely displaced by an excess of non-Myc-tagged rsCD146 (Fig. 1*C*). Finally, this binding was displaced by another binding partner of angiomotin, angiostatin (Fig. 1*D*).

Cell surface expression of angiomotin was observed by Western blot after plasma membrane extraction on both HUVEC and EPC (Fig. 2*A*). These results were confirmed by immunofluorescence experiments on migrating EPC (Fig. 2*B*). A membrane and intracellular labeling of angiomotin was observed as
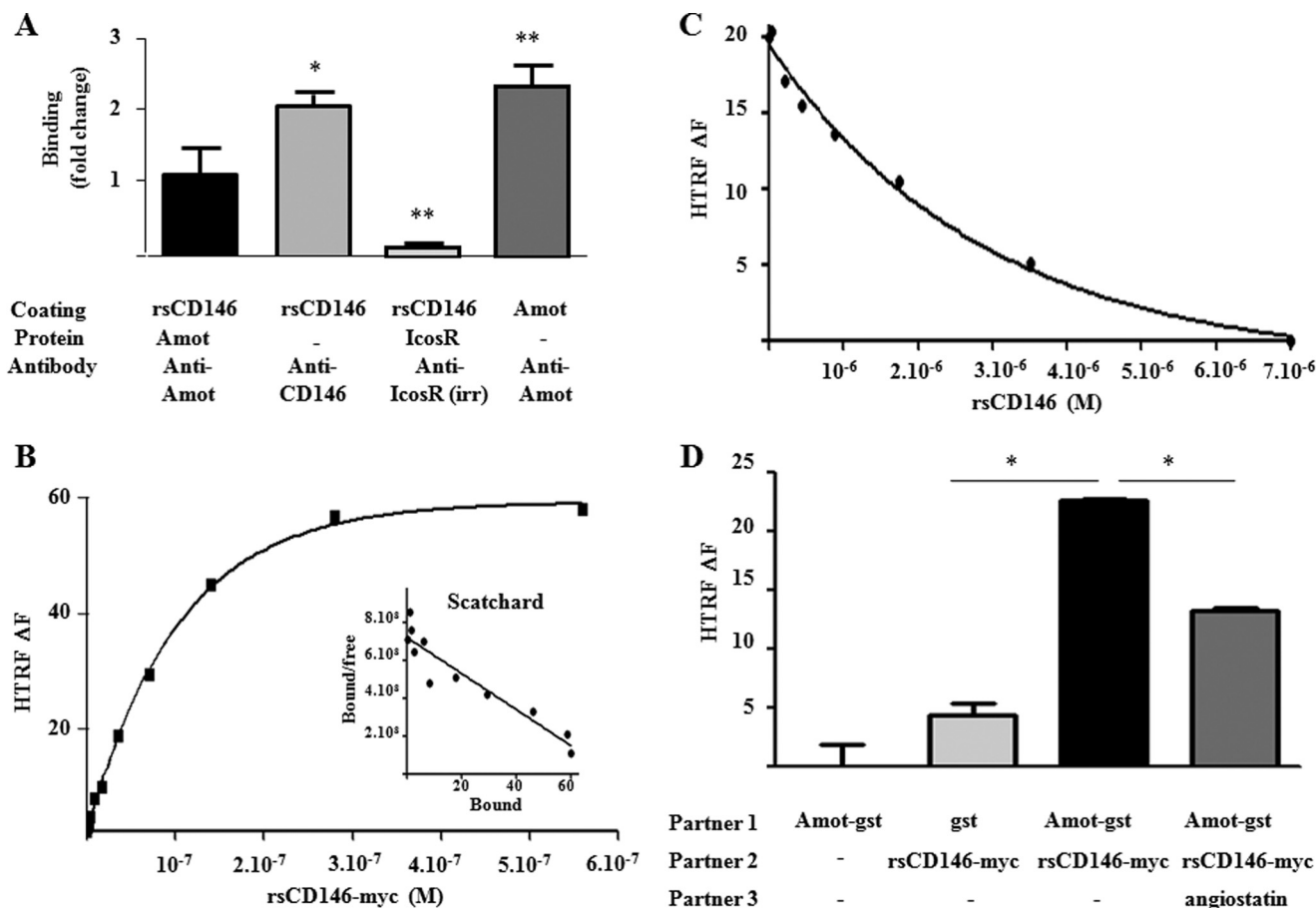
FIGURE 1. **Interaction between soluble CD146 and angiomotin.** *A*, association between rsCD146 and angiomotin in ELISA. Coating was performed with rsCD146 (1 $\mu$g/well) or angiomotin (*Amot*) (1 $\mu$g/well), and interaction was tested with Amot, anti-Amot, or an irrelevant protein (Icos receptor). Results are mean values of three experiments. *, $p < 0.05$; **, $p < 0.01$, experimental *versus* rsCD146/Amot condition. *B*, interaction between rsCD146-Myc and angiomotin-GST by HTRF assay. $4 \times 10^{-9}$ angiomotin-GST was incubated overnight at 4 °C with different concentrations of rsCD146-Myc ($5.5 \times 10^{-10}$-$5.5 \times 10^{-7}$ M) and second antibodies (anti-GST coupled to europium cryptate, $1.6 \times 10^{-9}$ M, and anti-Myc coupled to d2, $2.4 \times 10^{-8}$ M). Fluorescence intensity (HTRF $\Delta$F) was then measured using a microplate reader. A representative experiment of three different experiments is given with a nonlinear fit corresponding to one binding site ($r^2 = 0.9988$). The Scatchard plot is also given. The regression line corresponding to this Scatchard plot is $y = -0.9515 \times 10^7 \times +7.2 \times 10^8$. The estimated dissociation constant is $1.05 \times 10^{-7}$ M. *C*, displacement of rsCD146-Myc/angiomotin-GST interaction by rsCD146 in HTRF assay. $4 \times 10^{-9}$ M angiomotin-GST was incubated overnight at 4 °C with $1.4 \times 10^{-7}$ M rsCD146-Myc in the presence of different concentrations of non-tagged rsCD146 ($1.4 \times 10^{-8}$-$7 \times 10^{-6}$ M) and second antibodies coupled to europium cryptate or d2 (see *B*). Fluorescence intensity (HTRF $\Delta$F) was then measured using a microplate reader. A representative experiment of three different experiments is given with a nonlinear fit corresponding to competition on one binding site ($r^2 = 0.9950$). *D*, specificity of rsCD146-Myc/angiomotin-GST interaction in HTRF assay. $4 \times 10^{-9}$ M angiomotin-GST (*Amot-gst*) or GST was incubated overnight at 4 °C with or without $1.4 \times 10^{-7}$ M rsCD146-Myc in the presence or absence of $3.3 \times 10^{-6}$ M angiostatin and second antibodies coupled to europium cryptate or d2 (see *B*). Fluorescence intensity (HTRF $\Delta$F) was then measured using a microplate reader. Results are the mean value of four different experiments. *, $p < 0.05$, experimental *versus* control.

described previously (9). Surprisingly, angiomotin labeling was also observed in the nucleus, and this labeling was specific (see Fig. 2*C*). Both angiomotin and angiostatin localized at the cell surface of migrating EPC, and a similar localization was observed for rsCD146 (Fig. 2*B*). When angiomotin was silenced, the cell surface binding of both angiostatin and rsCD146 was abolished (Fig. 2*C*).

Using rAmot coupled to magnetic beads, flow cytometry experiments demonstrated that rsCD146, as angiostatin, was able to bind rAmot (Fig. 3*A*), whereas binding was lacking on magnetic beads in the absence of rAmot (data not shown). Recombinant sCD146 was also able to bind both HUVEC and EPC (Fig. 3*B*). In both cell types, the binding of rsCD146-FITC was significantly displaced by an equimolar concentration of angiostatin (Fig. 3*B*). In EPC in which angiomotin was silenced, binding of rsCD146 and angiostatin was significantly reduced (Fig. 3*C*). Finally, rsCD146 was able to bind HeLa cells trans-

fected with the angiogenic isoform of angiomotin, whereas it was unable to bind wild-type HeLa cells, which do not express the protein (Fig. 3*D*).

*Functional Consequences of the Binding of Soluble CD146 on Angiomotin*—To analyze the functional implication of angiomotin in sCD146 effects, we investigated whether angiomotin silencing was able to prevent angiogenesis induced by sCD146 in EPC. To this end, we evaluated the effects of 50 ng/ml rsCD146 on EPC after angiomotin siRNA transfection. When EPC were seeded on Matrigel plugs (Fig. 4*A*), rsCD146 addition led to a significant increase in tube number. In contrast, when EPC were silenced for angiomotin and treated with rsCD146, no increase was observed. The absence of effect of rsCD146 after angiomotin silencing was also observed in migration and proliferation experiments (Fig. 4*A*). Incubation of the cells with an excess of exogenous rAmot or with angiostatin (1 $\mu$g/ml) blocked the effect of rsCD146 on EPC proliferation (Fig. 4*B*).
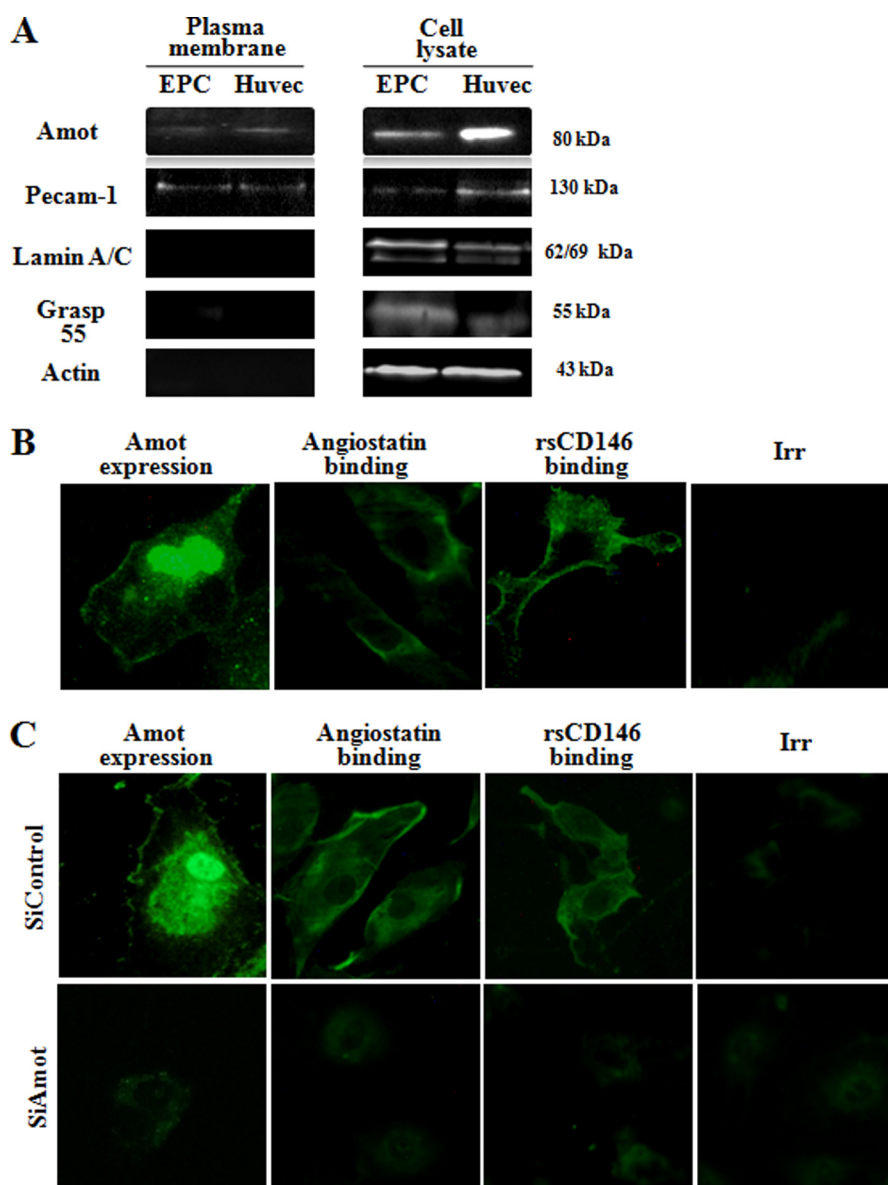
FIGURE 2. **Localization of angiomotin, angiostatin, and sCD146 on endothelial cells.** *A*, expression of angiomotin on the plasma membrane of EPC and HUVEC. Expression of 80-kDa angiomotin is visualized by Western blot in plasma membrane and cell lysate of both cell types. In these experiments, purity of the plasma membrane fraction was demonstrated by the absence of the nuclear membrane protein lamin and of the Golgi membrane protein grasp55 but the presence of the plasma membrane pecam-1. All these proteins were present in the whole cell lysate. *B*, visualization of sCD146 and angiostatin binding in migrating EPC. Immunofluorescence experiments were performed on EPC to confirm angiomotin expression at the cell membrane. An intracellular and nuclear labeling is also observed (permeabilized EPC). Angiostatin and rsCD146 binding were also visualized on non-permeabilized migrating EPC using angiostatin/anti-angiostatin antibody/secondary antibody-FITC and rsCD146-FITC, respectively. Isotypic control (*Irr-FITC*) was used. A representative experiment of three experiments is given. Magnification, ×40. *C*, absence of sCD146 and angiostatin binding in angiomotin-silenced EPC. Angiomotin silencing was visualized by the absence of expression of the molecule. Binding of angiostatin/anti-angiostatin antibody/secondary antibody-FITC and rsCD146-FITC was absent in angiomotin-silenced EPC as compared with control siRNA. Isotypic control (*Irr-FITC*) was used. Pictures are representative of three to four experiments. Magnification, ×40.

We previously described that an important effect of rsCD146 was the induction of eNOS transcription (5). This effect was blocked both in angiomotin-silenced EPC (Fig. 2*C*) and in EPC pretreated with 1 μg/ml angiostatin (Fig. 4*D*).

*Signaling Cascade Elicited by the Binding of Soluble CD146 on Angiomotin*—To gain insight into the signaling cascade elicited by the binding of soluble CD146 on angiomotin, we performed antibody arrays on EPC-treated or not with rsCD146. Results show that numerous proteins involved in different signaling pathways were either up- or down-regulated after rsCD146 treatment (Fig. 5*A*). Among the up-regulated pro-

teins, we observed p-Fak (×3.6), p-Akt (×2.6), and p-Jnk (×1.6). Western blot experiments confirmed that these proteins were effectively up-regulated 24 h after rsCD146 treatment (Fig. 5*B*). To confirm the involvement of angiomotin in the mechanism of action of soluble CD146, we examined the effect of rsCD146 on the induction of these proteins in angiomotin-silenced EPC. As expected, the effect was absent when angiomotin was silenced (Fig. 5*B*). Finally, as p-p38 has been reported to be increased in CD146-transfected endothelial cells (10), we also tested the effect of rsCD146 on this protein. Likewise, it was up-regulated, and the effect was abolished in angi-
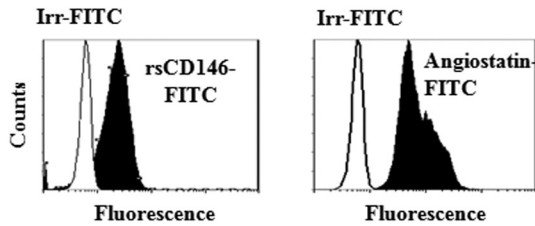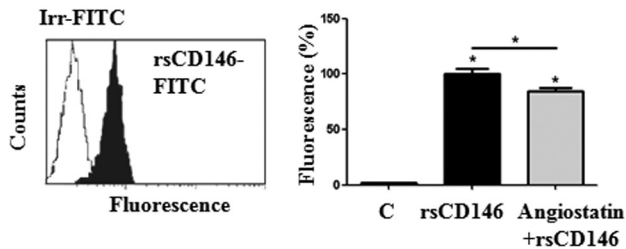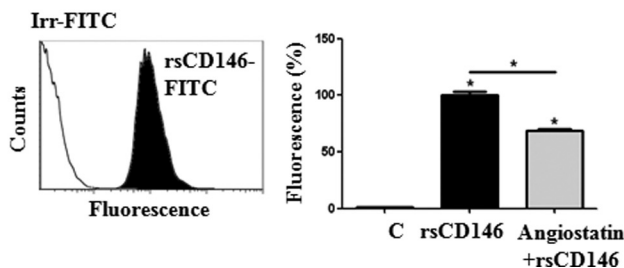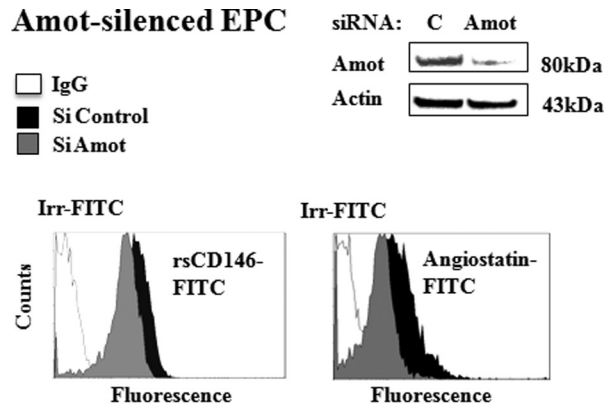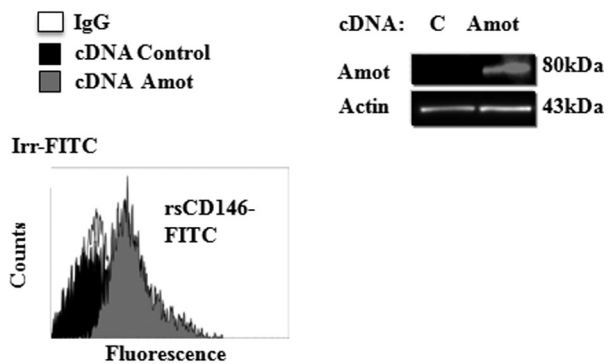
FIGURE 3. **Binding of angiomotin, angiostatin, and sCD146 on endothelial cells.** *A*, binding of sCD146 on recombinant angiomotin. Recombinant angiomotin was coupled to Dynabeads through an anti-GST antibody (see "Experimental Procedures"). Interaction of the molecule with rsCD146-FITC (1.5 $\mu$M) or angiostatin (1.5 $\mu$M) coupled to anti-angiostatin antibody and secondary antibody was tested by flow cytometry. Isotypic control (*Irr-FITC*) was used. A representative experiment of three to five experiments is given. *B*, binding of sCD146 on HUVEC and EPC. Binding of rsCD146-FITC (1.5 $\mu$M) was observed on HUVEC or EPC by flow cytometry. Isotypic control (*Irr-FITC*) was used. The rsCD146-FITC binding was displaced by an equimolar concentration of angiostatin. A representative experiment is given for the flow cytometry graph and displacement by angiostatin is the average of three to five experiments. *, $p < 0.05$, experimental *versus* control. *C*, reduced sCD146 binding in angiomotin-silenced EPC. Binding of rsCD146-FITC (1.5 $\mu$M) was observed by flow cytometry in EPC silenced or not for angiomotin. Angiomotin silencing was visualized by Western blot. The binding of angiostatin (1.5 $\mu$M) was also tested. Isotypic control (*Irr-FITC*) was used. A representative experiment of three experiments is shown. *D*, enhanced sCD146 binding in angiomotin-transfected HeLa cells. Binding of rsCD146-FITC (1.5 $\mu$M) was observed by flow cytometry in HeLa cells transfected with angiomotin. Angiomotin was not expressed in wild-type HeLa but was expressed after angiomotin transfection, as visualized by Western blot. Isotypic control (*Irr-FITC*) was used. A representative experiment of three experiments is shown.

omotin-silenced cells (Fig. 5*B*). In view of the major roles of the Fak and Akt pathways in cell migration and proliferation, respectively, we tested their involvement in these cellular functions elicited by rsCD146 by using specific inhibitors of these proteins. Results show that the Fak inhibitor 14 prevented the rsCD146-induced increase in EPC migration and that the Akt inhibitor GSK 690693 blocked the rsCD146-induced effect on EPC proliferation (Fig. 5*B*, *inset*).

## DISCUSSION

In this study, we identified angiomotin as an interacting partner of soluble CD146, mediating its angiogenic effects in EPC. Initially, angiomotin has been identified in a yeast two-hybrid screen by its ability to bind angiostatin, a circulating inhibitor of blood vessels formation (9). Angiomotin is a membrane-associated protein expressed on human endothelium that promotes angiogenesis by controlling directional migration (11, 12). Accordingly, therapeutic antibodies targeting angiomotin have

been shown to inhibit angiogenesis both *in vitro* and *in vivo* (13). At the structural level, angiomotin presents conserved coiled-coil and PDZ binding domains (14) Taken together, the data suggest that angiomotin could be constitutive of an intracellular molecular scaffold network regulated by both the circulating angiostatin and sCD146.

Using different approaches, we have shown that sCD146 is able to bind angiomotin. This binding is specific and can be partially displaced by an equimolar amount of angiostatin. HTRF experiments with recombinant proteins allowed to estimate the dissociation constant $\sim 10^{-7}$ M. In comparison, the dissociation constants observed for the interaction of angiostatin with two angiostatin-binding proteins, soluble c-Met (15) and ORF (16), are $7.5 \times 10^{-7}$ M and $3.4 \times 10^{-7}$ M, respectively. The strength of the interaction between sCD146 and angiomotin is comparable or slightly less than those reported for the interaction between receptors and ligands (17) or antigens and antibodies (18) and corresponds to that described for general
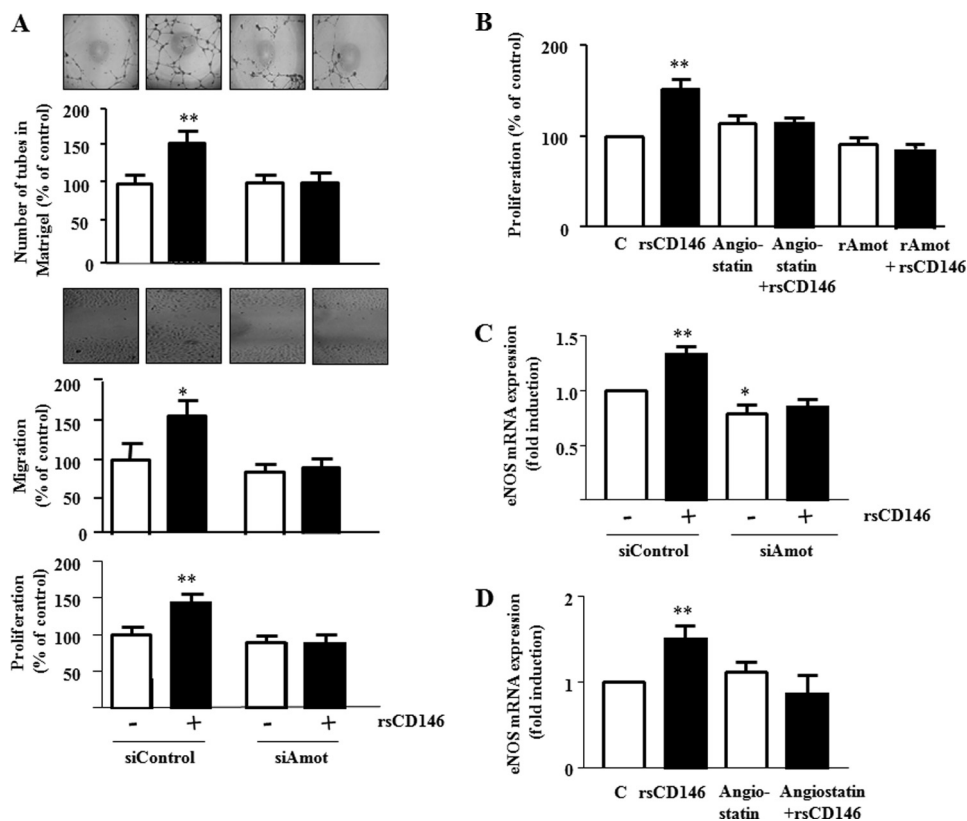
FIGURE 4. **Angiomotin mediates the angiogenic effects of soluble CD146.** *A*, absence of angiogenic effect of sCD146 in EPC silenced for angiomotin. The influence of angiomotin siRNA was evaluated on the effect of rsCD146 (50 ng/ml) on pseudocapillaries formation in Matrigel (*upper panel*), migration (*middle panel*), and proliferation (*lower panel*) of EPC. Control siRNA (*siControl*) were used as controls. *Insets* show one representative experiment of tube formation in Matrigel and one representative experiment of migration after healing. Results are the mean values $\pm$ S.E. of five different experiments. *B*, angiostatin and extracellular angiomotin addition inhibit the effect of sCD146 on EPC proliferation. The effect of rsCD146 (50 ng/ml) on proliferation of EPC was evaluated after treatment of the cells with 1 $\mu$g/ml angiostatin (*Ang*) or addition of an excess of extracellular rAmot. Results are the mean values $\pm$ S.E. of five different experiments. *C*, angiomotin silencing in EPC inhibits the sCD146-induced increase in eNOS mRNA. The capacity of EPC to induce eNOS mRNA in response to rsCD146 (50 ng/ml) was evaluated after angiomotin silencing. Results are the mean values $\pm$ S.E. of four different experiments. *D*, angiostatin inhibits the sCD146-induced increase in eNOS mRNA in EPC. The capacity of EPC to induce eNOS mRNA in response to rsCD146 was evaluated after addition of angiostatin (*Ang*) (1 $\mu$g/ml). Results are the mean values $\pm$ S.E. of four different experiments. *, $p < 0.05$; **, $p < 0.01$, experimental *versus* control (*C*).

protein-protein interactions with a $K_d$ value in the range of $10^{-6}$–$10^{-7}$ M (19).

Two isoforms of angiomotin, generated by alternate splicing, have been described (20). They display differential roles in the switch between migration and stabilization of endothelial cells. One isoform (80 kDa) is responsible for the migratory and angiogenic functions of the protein whereas the second (130 kDa), localized at the tight junction of confluent cells, is involved in the stabilization and maturation functions (20). The relative expression levels of p80 and p130 isoforms regulate the switch between the migratory and mature cell phenotypes. In migratory cells, the p80 isoform is the mainly expressed isoform. In this study, we focused on angiogenic functions of sCD146 in migrating EPC and observed effects that are mediated through the angiogenic 80-kDa isoform. However, as the extracellular part of the molecule, which contains the angiostatin binding domain, is common to the two isoforms, we can assume that sCD146 is able to interact with both proteins. In the future, it will be interesting to differentiate the selective effects of sCD146 on the two isoforms as the function of the phenotype of the cells, migratory or stabilized in an endothelial monolayer.

Angiostatin has been shown to potently inhibit angiogenesis and metastasis in mice (21). *In vitro* studies have shown that

angiostatin can inhibit endothelial cell proliferation (21) and migration (22) and induces apoptosis (23, 24). In a recent study, we have described opposite properties for sCD146 (5). Because angiomotin is able to interact with both molecules, angiostatin and sCD146 could constitute negative and positive regulators of angiomotin, respectively. The angiogenic activity of the cell could thus be modulated as a function of the physiological need by the balance between both circulating molecules. Because angiostatin was able to displace sCD146 binding in our experiments, it will be of interest to examine whether the binding domains of angiostatin and sCD146 on the extracellular part of angiomotin are different or overlapping.

Although it has been reported that CD146 acts as a homophilic adhesion molecule, we (4) and others (25) have not been able to show a direct interaction between sCD146 and membrane CD146 or between membrane CD146 and itself. Along this line, two different heterophilic ligands of membrane CD146 have been recently described. Thus, Flanagan *et al.* (25) have shown that laminin-411 binds membrane CD146 to facilitate TH17 cell entry into the tissues and promote inflammation. Jouve *et al.* (26) have recently reported that galectin-1 directly binds membrane CD146 and that this interaction is involved in the control of endothelial cell apoptosis. In the present study, we also showed that soluble CD146 acts as a hetero-
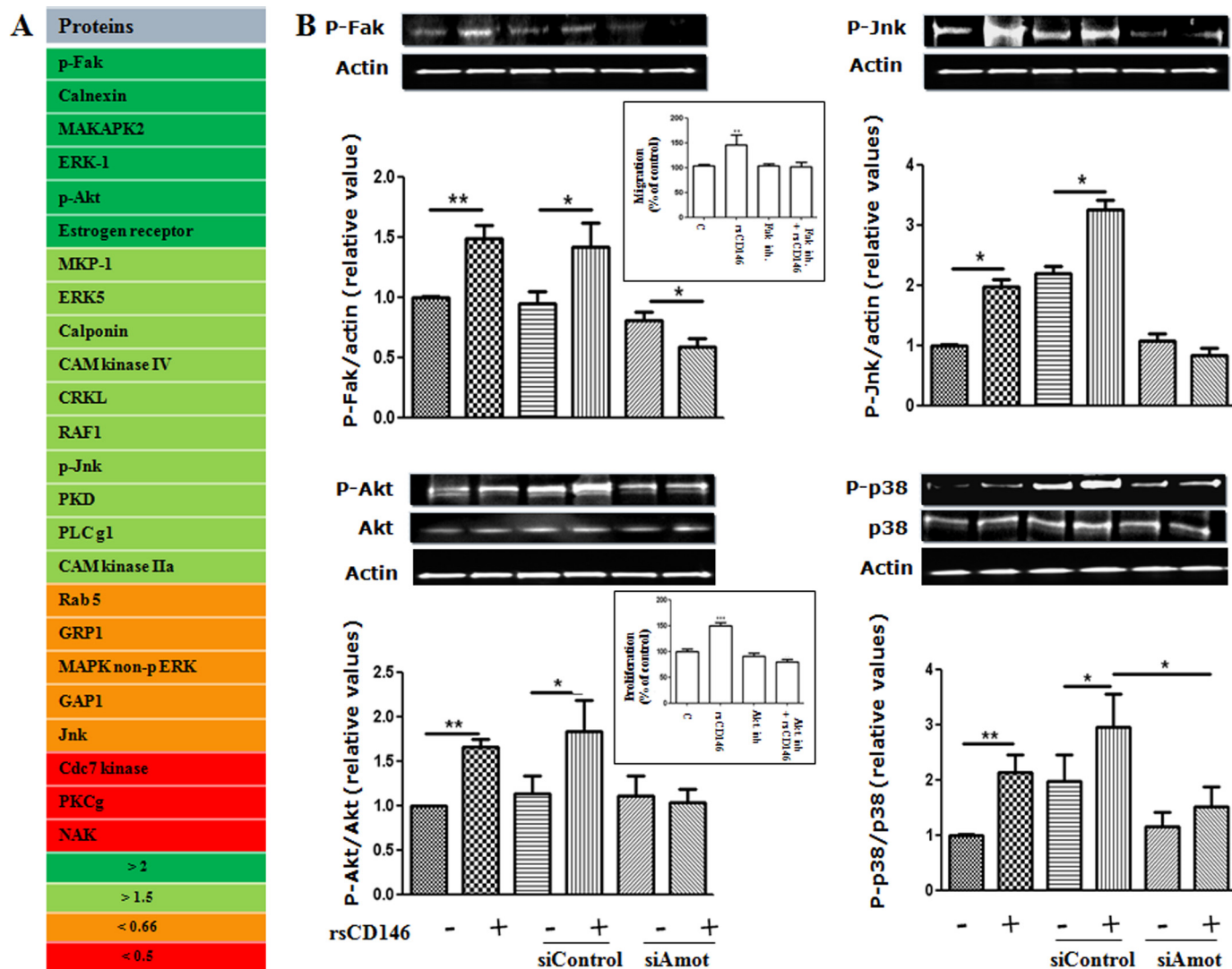
FIGURE 5. **Involvement of angiomotin in the signaling cascade elicited by soluble CD146 in endothelial progenitor cells.** *A*, analysis of signal transduction proteins modulated in response to rsCD146. Proteins that were up- or down-regulated in response to rsCD146 were characterized by antibody array (see "Experimental Procedures"). Proteins were classified as a function of the induction factor ($>2$ or $>1.5$) or the inhibition factor ($<0.66$ or $<0.5$), as compared with control condition. *B*, induction of p-Fak, p-Jnk, p-Akt, and p-p38 in response to rsCD146. The effect or rsCD146 was analyzed by Western blot and quantified. The effect of angiomotin silencing was also tested. A representative experiment is presented for each protein, and the average of three to six experiments is given. In the *inset* are shown the inhibitory effects of the Fak inhibitor 14 and of the Akt inhibitor GSK 690693 on the rsCD146-induced increase in EPC migration and proliferation, respectively. *, $p < 0.05$; **, $p < 0.01$, experimental *versus* control (*C*).

philic ligand binding to angiomotin. Altogether, these results suggest that both soluble and membrane CD146 are able to bind different proteins as a function of the cellular and physiopathological context but that heterophilic interactions are favored. Of interest, we found angiomotin mRNA expression (data not shown) not only in endothelial cells as HUVEC and EPC but also in the trophoblastic cell line HTR-8/SVneo, in L929 fibroblastic cells and in the monocytic cell line THP1, which does not express membrane CD146 but was activated by sCD146 during transmigration (4). Identifying angiomotin expressing cells will presumably provide new target cells for sCD146.

Using antibody array, we examined the signaling cascade elicited by angiomotin following sCD146 binding. We observed that p-Fak, p-Akt, and p-Jnk were up-regulated by sCD146 binding and that the effect was mediated through angiomotin. Likewise, p-p38 was also up-regulated. Of interest, the sCD146-

induced increase in EPC migration and proliferation were prevented by the Fak inhibitor 14 and the Akt inhibitor GSK 690693, respectively, demonstrating a direct involvement of these signaling pathways in the mechanism of action of sCD146. These results are in accordance with data of the literature. Indeed, it was shown by our team that activation of human endothelial cells via S-endo-1 antigen (CD146) stimulates the tyrosine phosphorylation of focal adhesion kinase p125 (Fak) (27). Likewise, a reciprocal regulation of MelCAM and Akt has been described in human melanoma (28). Finally, biochemical studies revealed that CD146 was required for the activation of p38/IKK/NF$\kappa$B signaling cascade and up-regulation of NF$\kappa$B downstream proangiogenic genes in response to tumor secretions (29). Examination of the angiomotin structure shows that it is lacking catalytic motifs and can therefore apparently not transduce signals by itself. We can thus assume that angiomotin could act as a co-receptor, generating a com-

plex with a corresponding surface receptor to regulate signaling and/or as a scaffold protein interacting, in particular through its PDZ binding domain, with other proteins transducing the signal. Two studies have shown that angiomotin is able to participate to protein complexes involved in the transduction of intracellular signals. Thus, angiomotin was reported to bind Rich1, a Rho-GTPase-activating protein, and to a complex containing the PDZ-domain proteins Pals1, Patj, and Par-3 (30). Likewise, the angiomotin-Patj-Syx signaling complex was shown to spatially control RhoA-GTPase activity in migrating endothelial cells (31). Finally, a merlin-angiomotin complex was identified that mediates the regulation of mitogenic signaling (32). The finding of the different proteins constituting, in association with angiomotin, the signalosome activated by sCD146 will be the aim of future studies. Of interest, Jiang *et al.* (33) reported in a recent study that CD146 is a co-receptor for VEGFR-2 in tumor angiogenesis. Indeed, CD146 directly interacts with VEGFR-2 on endothelial cells as well as at the molecular level. In addition, they show that CD146 is required in the VEGF-induced VEGFR-2 phosphorylation and Akt/p38, MAPK/NF-$\kappa$B activation. Here, we show that sCD146, through its binding to angiomotin, induces the activation of several signaling pathways, with the phosphorylation of Fak, Akt, Jnk, and p38. Whether the activation of these pathways through angiomotin requires the involvement of membrane CD146 and/or VEGFR2 remains to be elucidated, but it appears clearly from our experiments that both VEGF and sCD146 could act on several common signaling pathways.

Taken together, we present here a novel signaling pathway involving sCD146 and the membrane-associated angiomotin. Given the role of sCD146 and angiostatin (34, 35) in ischemic diseases, this work will open up new ways to either activate or inhibit EPC during pathological conditions (36).

## REFERENCES

1. Bardin, N., Reumaux, D., Geboes, K., Colombel, J. F., Blot-Chabaud, M., Sampol, J., Duthilleul, P., and Dignat-George, F. (2006) Increased expression of CD146, a new marker of the endothelial junction in active inflammatory bowel disease. *Inflamm. Bowel Dis.* **12,** 16–21
2. Pasquier, E., Bardin, N., De Saint Martin, L., Le Martelot, M. T., Bohec, C., Roche, S., Mottier, D., and Dignat-George, F. (2005) The first assessment of soluble CD146 in women with unexplained pregnancy loss. A new insight? *Thromb. Haemost.* **94,** 1280–1284
3. Bardin, N., Moal, V., Anfosso, F., Daniel, L., Brunet, P., Sampol, J., and Dignat George, F. (2003) Soluble CD146, a novel endothelial marker, is increased in physiopathological settings linked to endothelial junctional alteration. *Thromb. Haemost.* **90,** 915–920
4. Bardin, N., Blot-Chabaud, M., Despoix, N., Kebir, A., Harhouri, K., Arsanto, J. P., Espinosa, L., Perrin, P., Robert, S., Vely, F., Sabatier, F., Le Bivic, A., Kaplanski, G., Sampol, J., and Dignat-George, F. (2009) CD146 and its soluble form regulate monocyte transendothelial migration. *Arterioscler. Thromb. Vasc. Biol.* **29,** 746–753
5. Harhouri, K., Kebir, A., Guillet, B., Foucault-Bertaud, A., Voytenko, S., Piercecchi-Marti, M. D., Berenguer, C., Lamy, E., Vely, F., Pisano, P., Ouafik, L., Sabatier, F., Sampol, J., Bardin, N., Dignat-George, F., and Blot-Chabaud, M. (2010) Soluble CD146 displays angiogenic properties and promotes neovascularization in experimental hind-limb ischemia. *Blood* **115,** 3843–3851
6. Almeras, L., Eyles, D., Benech, P., Laffite, D., Villard, C., Patatian, A., Boucraut, J., Mackay-Sim, A., McGrath, J., and Féron, F. (2007) Developmental vitamin D deficiency alters brain protein expression in the adult rat: implications for neuropsychiatric disorders. *Proteomics.* **7,** 769–780
7. Delorme, B., Basire, A., Gentile, C., Sabatier, F., Monsonis, F., Desouches, C., Blot-Chabaud, M., Uzan, G., Sampol, J., and Dignat-George, F. (2005) Presence of endothelial progenitor cells, distinct from mature endothelial cells, within human CD146+ blood cells. *Thromb. Haemost.* **94,** 1270–1279
8. Kebir, A., Harhouri, K., Guillet, B., Liu, J. W., Foucault-Bertaud, A., Lamy, E., Kaspi, E., Elganfoud, N., Vely, F., Sabatier, F., Sampol, J., Pisano, P., Kruithof, E. K., Bardin, N., Dignat-George, F., and Blot-Chabaud, M. (2010) CD146 short isoform increases the proangiogenic potential of endothelial progenitor cells *in vitro* and *in vivo*. *Circ. Res.* **107,** 66–75
9. Troyanovsky, B., Levchenko, T., Månsson, G., Matvijenko, O., and Holmgren, L. (2001) Angiomotin: an angiostatin binding protein that regulates endothelial cell migration and tube formation. *J. Cell Biol.* **152,** 1247–1254
10. Zheng, C., Qiu, Y., Zeng, Q., Zhang, Y., Lu, D., Yang, D., Feng, J., and Yan, X. (2009) Endothelial CD146 is required for *in vitro* tumor-induced angiogenesis: the role of a disulfide bond in signaling and dimerization. *Int. J. Biochem. Cell Biol.* **41,** 2163–2172
11. Bratt, A., Birot, O., Sinha, I., Veitonmäki, N., Aase, K., Ernkvist, M., and Holmgren, L. (2005) Angiomotin regulates endothelial cell-cell junctions and cell motility. *J. Biol. Chem.* **280,** 34859–34869
12. Aase, K., Ernkvist, M., Ebarasi, L., Jakobsson, L., Majumdar, A., Yi, C., Birot, O., Ming, Y., Kvanta, A., Edholm, D., Aspenström, P., Kissil, J., Claesson-Welsh, L., Shimono, A., and Holmgren, L. (2007) Angiomotin regulates endothelial cell migration during embryonic angiogenesis. *Genes Dev.* **21,** 2055–2068
13. Holmgren, L., Ambrosino, E., Birot, O., Tullus, C., Veitonmäki, N., Levchenko, T., Carlson, L. M., Musiani, P., Iezzi, M., Curcio, C., Forni, G., Cavallo, F., and Kiessling, R. (2006) A DNA vaccine targeting angiomotin inhibits angiogenesis and suppresses tumor growth. *Proc. Natl. Acad. Sci. U.S.A.* **103,** 9208–9213
14. Bratt, A., Wilson, W. J., Troyanovsky, B., Aase, K., Kessler, R., Van Meir, E. G., and Holmgren, L. (2002) Angiomotin belongs to a novel protein family with conserved coiled-coil and PDZ binding domains. *Gene* **298,** 69–77
15. Wajih, N., and Sane, D. C. (2003) Angiostatin selectively inhibits signaling by hepatocyte growth factor in endothelial and smooth muscle cells. *Blood* **101,** 1857–1863
16. Kang, H. T., Bang, W. K., and Yu, Y. G. (2004) Identification and characterization of a novel angiostatin-binding protein by the display cloning method. *J. Biochem. Mol. Biol.* **37,** 159–166
17. Cochrane, D., Webster, C., Masih, G., and McCafferty, J. (2000) Identification of natural ligands for SH2 domains from a phage display cDNA library. *J. Mol. Biol.* **297,** 89–97
18. Daugherty, P. S., Chen, G., Olsen, M. J., Iverson, B. L., and Georgiou, G. (1998) Antibody affinity maturation using bacterial surface display. *Protein Eng.* **11,** 825–832
19. Causey, L. D., and Dwyer, D. S. (1996) Detection of low affinity interactions between peptides and heat shock proteins by chemiluminescence of enhanced avidity reactions (CLEAR). *Nat. Biotechnol.* **14,** 348–351
20. Ernkvist, M., Birot, O., Sinha, I., Veitonmaki, N., Nyström, S., Aase, K., and Holmgren, L. (2008) Differential roles of p80- and p130-angiomotin in the switch between migration and stabilization of endothelial cells. *Biochim. Biophys. Acta* **1783,** 429–437
21. O'Reilly, M. S., Holmgren, L., Shing, Y., Chen, C., Rosenthal, R. A., Moses, M., Lane, W. S., Cao, Y., Sage, E. H., and Folkman, J. (1994) Angiostatin: a novel angiogenesis inhibitor that mediates the suppression of metastases by a Lewis lung carcinoma. *Cell* **79,** 315–328
22. Ji, W. R., Castellino, F. J., Chang, Y., Deford, M. E., Gray, H., Villarreal, X., Kondri, M. E., Marti, D. N., Llinás, M., Schaller, J., Kramer, R. A., and Trail, P. A. (1998) Characterization of kringle domains of angiostatin as antag-

onists of endothelial cell migration, an important process in angiogenesis. *FASEB J.* **12,** 1731–1738

23. Claesson-Welsh, L., Welsh, M., Ito, N., Anand-Apte, B., Soker, S., Zetter, B., O'Reilly, M., and Folkman, J. (1998) Angiostatin induces endothelial cell apoptosis and activation of focal adhesion kinase independently of the integrin-binding motif RGD. *Proc. Natl. Acad. Sci. U.S.A.* **95,** 5579–5583

24. Lucas, R., Holmgren, L., Garcia, I., Jimenez, B., Mandriota, S. J., Borlat, F., Sim, B. K., Wu, Z., Grau, G. E., Shing, Y., Soff, G. A., Bouck, N., and Pepper, M. S. (1998) Multiple forms of angiostatin induce apoptosis in endothelial cells. *Blood* **92,** 4730–4741

25. Flanagan, K., Fitzgerald, K., Baker, J., Regnstrom, K., Gardai, S., Bard, F., Mocci, S., Seto, P., You, M., Larochelle, C., Prat, A., Chow, S., Li, L., Vandevert, C., Zago, W., Lorenzana, C., Nishioka, C., Hoffman, J., Botelho, R., Willits, C., Tanaka, K., Johnston, J., and Yednock, T. (2012) Laminin-411 is a vascular ligand for MCAM and facilitates TH17 cell entry into the CNS. *PLoS One* **7,** e40443

26. Jouve, N., Despoix, N., Espeli, M., Gauthier, L., Cypowyj, S., Fallague, K., Schiff, C., Dignat-George, F., Vely, F., and Leroyer, A. (2013) The involvement of CD146 and its novel ligand Galectin-1 in apoptotic regulation of endothelial cells. *J. Biol. Chem.* **288,** 2571–2579

27. Anfosso, F., Bardin, N., Francès, V., Vivier, E., Camoin-Jau, L., Sampol, J., and Dignat-George, F. (1998) Activation of human endothelial cells via S-endo-1 antigen (CD146) stimulates the tyrosine phosphorylation of focal adhesion kinase p125(FAK). *J. Biol. Chem.* **273,** 26852–26856

28. Li, G., Kalabis, J., Xu, X., Meier, F., Oka, M., Bogenrieder, T., and Herlyn, M. (2003) Reciprocal regulation of MelCAM and AKT in human melanoma. *Oncogene* **22,** 6891–6899

29. Bu, P., Gao, L., Zhuang, J., Feng, J., Yang, D., and Yan, X. (2006) Anti-CD146 monoclonal antibody AA98 inhibits angiogenesis via suppression of nuclear factor-kappaB activation. *Mol. Cancer Ther.* **5,** 2872–2878

30. Wells, C. D., Fawcett, J. P., Traweger, A., Yamanaka, Y., Goudreault, M., Elder, K., Kulkarni, S., Gish, G., Virag, C., Lim, C., Colwill, K., Starostine, A., Metalnikov, P., and Pawson, T. (2006) A Rich1/Amot complex regulates the Cdc42 GTPase and apical-polarity proteins in epithelial cells. *Cell* **125,** 535–548

31. Ernkvist, M., Luna Persson, N., Audebert, S., Lecine, P., Sinha, I., Liu, M., Schlueter, M., Horowitz, A., Aase, K., Weide, T., Borg, J. P., Majumdar, A., and Holmgren, L. (2009) The Amot/Patj/Syx signaling complex spatially controls RhoA GTPase activity in migrating endothelial cells. *Blood* **113,** 244–253

32. Yi, C., Troutman, S., Fera, D., Stemmer-Rachamimov, A., Avila, J. L., Christian, N., Persson, N. L., Shimono, A., Speicher, D. W., Marmorstein, R., Holmgren, L., and Kissil, J. L. (2011) A tight junction-associated Merlin-angiomotin complex mediates Merlin's regulation of mitogenic signaling and tumor suppressive functions. *Cancer Cell* **19,** 527–540

33. Jiang, T., Zhuang, J., Duan, H., Luo, Y., Zeng, Q., Fan, K., Yan, H., Lu, D., Ye, Z., Hao, J., Feng, J., Yang, D., and Yan, X. (2012) CD146 is a coreceptor for VEGFR-2 in tumor angiogenesis. *Blood* **120,** 2330–2339

34. Matsunaga, T., Chilian, W. M., and March, K. (2005) Angiostatin is negatively associated with coronary collateral growth in patients with coronary artery disease. *Am. J. Physiol. Heart Circ. Physiol.* **288,** H2042–6

35. Basile, D. P., Fredrich, K., Weihrauch, D., Hattan, N., and Chilian, W. M. (2004) Angiostatin and matrix metalloprotease expression following ischemic acute renal failure. *Am. J. Physiol. Renal Physiol.* **286,** F893–902

36. Pearson, J. D. (2009) Endothelial progenitor cells - hype or hope? *J. Thromb. Haemost.* **7,** 255–262